

MICROCOPY RESOLUTION TEST CHART
NATIONAL BUREAU OF STANDARDS-1963-A

AD-A143 664

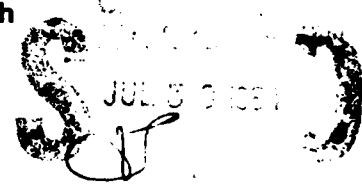
MONOLITHIC SAW OSCILLATORS ON SILICON

FINAL REPORT FOR THE PERIOD
September 15, 1982 through September 14, 1983

CONTRACT NO. F49620-82-C-0094

Sponsored by

Air Force Office of Scientific Research
Bolling Air Force Base
Washington, DC 20332



M.E. Motamedi
Program Manager

Approved for public release
distribution unlimited

APRIL 1984

DHC FILE COPY

This manuscript is submitted for publication with the understanding that the United States Government is authorized to reproduce and distribute reprints for governmental purposes.



Rockwell International

84 07 24 026

UNCLASSIFIED

SECURITY CLASSIFICATION OF THIS PAGE

REPORT DOCUMENTATION PAGE

1a. REPORT SECURITY CLASSIFICATION Unclassified		1b. RESTRICTIVE MARKINGS	
2a. SECURITY CLASSIFICATION AUTHORITY		3. DISTRIBUTION/AVAILABILITY OF REPORT Approved for public release; distribution unlimited.	
2b. DECLASSIFICATION/DOWNGRADING SCHEDULE			
4. PERFORMING ORGANIZATION REPORT NUMBER(S) MRDC41125.1FR		5. MONITORING ORGANIZATION REPORT NUMBER(S) AFOSR-TR. 34 0557	
6a. NAME OF PERFORMING ORGANIZATION Rockwell International Microelectronics Research and Development Center	6b. OFFICE SYMBOL (If applicable)	7a. NAME OF MONITORING ORGANIZATION AFOSR/NE	
6c. ADDRESS (City, State and ZIP Code) 1049 Camino Dos Rios Thousand Oaks, California 91360		7b. ADDRESS (City, State and ZIP Code) Bldg 410 Bolling AFB DC 20332	
8a. NAME OF FUNDING/SPONSORING ORGANIZATION Air Force Office of Scientific Research	8b. OFFICE SYMBOL (If applicable) NE	8. PROCUREMENT INSTRUMENT IDENTIFICATION NUMBER Contract No. F49620-82-C-0094	
8c. ADDRESS (City, State and ZIP Code) Bolling Air Force Base Washington, D.C. 20332		10. SOURCE OF FUNDING NOS.	
11. TITLE (Include Security Classification) MONOLITHIC SAW OSCILLATORS ON SILICON (U)		PROGRAM ELEMENT NO. 61102F	PROJECT NO. 3306
12. PERSONAL AUTHOR(S) Motamedi, M.E.; Kilcoyne, M.K.		TASK NO. B2	WORK UNIT NO.
13a. TYPE OF REPORT Final Report	13b. TIME COVERED FROM 09/15/82 TO 09/14/83	14. DATE OF REPORT (Yr., Mo., Day) APRIL 1984	15. PAGE COUNT 46
16. SUPPLEMENTARY NOTATION			
17. COSATI CODES		18. SUBJECT TERMS (Continue on reverse if necessary and identify by block number)	
FIELD	GROUP	SUB. GR.	Monolithic SAW silicon resonator.
19. ABSTRACT (Continue on reverse if necessary and identify by block number)			
<p>In this report progress in development of a monolithic SAW silicon resonator is described. Specific studies and results in the areas of piezoelectric films for generation and detection of SAW are presented. A multi-mode SAW resonator using thin film ZnO on silicon was designed, fabricated and characterized. Methods were developed for a new technique of fabricating silicon SAW resonator cavity using orientational etching. It was concluded that this type of etching results in well-defined sidewall structures for reflector cavity element, producing a superior resonant performance with lower phase noise than conventional SAW resonators. Automated measurement equipment was employed to evaluate devices and confirm equivalent circuit models. Device performance very closely matched original circuit models showing excellent confirmation of design parameters.</p>			
20. DISTRIBUTION/AVAILABILITY OF ABSTRACT UNCLASSIFIED/UNLIMITED <input checked="" type="checkbox"/> SAME AS RPT. <input type="checkbox"/> DTIC USERS <input type="checkbox"/>		21. ABSTRACT SECURITY CLASSIFICATION Unclassified	
22a. NAME OF RESPONSIBLE INDIVIDUAL 1Lt Kevin J. Mallon		22b. TELEPHONE NUMBER (Include Area Code) 302-767-4931	22c. OFFICE SYMBOL NE

DD FORM 1473, 83 APR

EDITION OF 1 JAN 73 IS OBSOLETE.

UNCLASSIFIED
SECURITY CLASSIFICATION OF THIS PAGE

MRDC41125.1FR

TABLE OF CONTENTS

		PAGE
1.0	INTRODUCTION.	1
2.0	TECHNICAL APPROACH.	3
2.1	Thin Film SAW Resonator Design	4
2.1.1	Background.	4
2.1.2	Theory of Operation	6
2.1.3	Resonator Structure	7
2.1.4	Silicon Resonator High Frequency Advantages.	9
2.1.5	Device Modeling	11
2.1.6	Single Mode Resonator	13
2.1.7	Equivalent Circuit Models	19
2.1.8	Frequency Stability	23
2.2	Device Design.	25
2.3	Mask Design and Fabrication.	25
2.4	Resonator Fabrication.	28
2.5	Experimental Results	34
3.0	CONCLUSIONS	40
4.0	RECOMMENDATIONS FOR FUTURE EFFORTS.	42
5.0	REFERENCES.	46

Codes
and/or
Special
A-1



AIR FORCE QUALITY ASSURANCE

Chief, Technical Information Division



LIST OF FIGURES

	PAGE
1. SAW resonator cavity structures	10
2. Device frequency as a function of linewidth for different substrates.	12
3. General resonator structure and key parameters for design.	14
4. Equivalent circuits for SAW resonator	20
5. Amplitude and phase responses of a 500 MHz SAW resonator driven from the equivalent circuit model. . .	24
6. SAW one-port multi-mode resonator structure	26
7. Cross-sectional view of a one-port resonator after processing.	27
8. Computer plot of actual design superimposing all of the four mask layers.	29
9. IDT mask detail with cosine-hyperbolic-cosine weighting in the electrode structure.	30
10. SEM picture of a silicon resonator groove using anisotropic etching technique	32
11. SEM picture of a reflector cross-section using anisotropic etching technique	33
12. A portion of 3" silicon wafer containing 26 resonators with one device mounted in TO-8 package. . .	35
13. 50-ohm matched fixture is designed for resonator characterization after mounted in TO-8 package.	36
14. Experimental plot of return loss amplitude for a multi-mode silicon resonator.	37
15. Complete integration of a two-port silicon resonator	45

1.0 INTRODUCTION

Surface acoustic wave (SAW) devices provide special advantages in air defense systems^{1,2} which have proven invaluable to all branches of the military in all applications such as narrow-band high-gain low-noise receivers, stabilized reference oscillator sources, and sensor devices such as pressure sensors and accelerometers for navigation. Design flexibility of SAW devices has proven of vital importance in application where reliable, reproducible components featuring linear phase, temperature stability, small size and low power are required. SAW devices have been applied in the exacting requirements of modern military systems³ as delay lines, bandpass filters, resonators, oscillators, and other state-of-the-art signal processing applications where the specific properties of SAW devices provide special capabilities not available by any other means.

The particular types of SAW devices evaluated in this one-year study program involve thin film SAW resonator structures fabricated on silicon wafers. These devices use thin film piezoelectric materials and offer performance capabilities not possible with conventional bulk materials as well as the key advantage of direct integration with associated circuitry on a single monolithic chip. Resonator devices well in excess of 1GHz are easily possible on silicon monolithic substrates since the



MRDC41125.1FR

acoustic velocity is over 60% higher in silicon materials, thereby reducing high resolution geometry requirements in SAW devices by that factor. Success of the one-year study program has been greatly augmented by the existence of a complete SAW processing facility, including total in-house design and mask generation capability, clean room processing laboratories, and extensive measurement and analysis equipment for material characterization. This equipment includes Auger spectrometry, SIMS and ESCA analytical equipment, as well as laser RAMAN spectroscopy for analysis of surface strain conditions and substrate materials. This equipment, as well as our electronic measurements laboratory, give us a total capability of material analysis and electronic characterization of multi-mode resonance structures of SAW devices.

The following pages outline in detail our technical approach employed during this study as well as design and processing methods developed and experimental results and evaluations.



2.0 TECHNICAL APPROACH

The objective of this program is to perform the necessary research and development to evaluate feasibility, performance and high frequency limitations of thin film monolithic SAW oscillators processed on silicon substrates. Selection of silicon as a substrate material was based on its strong history as a semiconductor material and also on its low defect density, availability, and low cost. In considering future integration of electronic circuits with the SAW devices, many types of high frequency silicon transistors with excellent performance have already been developed.

The choice of silicon offered other advantages as well in processing thin film SAW devices. The anisotropic properties of silicon were used to advantage by etching extremely high definition reflector structures using a solution of ethylene diamine-pyrocatechol (EDP). This material has anisotropic properties as applied to silicon.⁴⁻⁶ The etching of silicon is influenced by: a) the crystallographic perfection of the substrate, b) the substrate surface, and c) the control exercised over the anisotropic etching conditions. Thermally grown silicon dioxide has been found to be an excellent masking film and is readily available. EDP etching is now routinely accomplished in our laboratories in a specially designed etching chamber where temperature and circulation are carefully controlled.



MRDC41125.1FR

Alternate approaches for anisotropic etching were also evaluated using both CF_4 and SF_6 . Although both were capable of anisotropic etching properties, the ratio of vertical to horizontal etching is not as well controlled as in EDP. EDP has the advantage that crystallographic structure is not the controlling factor with this type of etch.

2.1 THIN FILM SAW RESONATOR DESIGN

2.1.1 BACKGROUND

For the past ten years, surface acoustic wave oscillators have been competing as alternative IF frequency sources to bulk wave crystal oscillators.^{7,8} They are currently used in numerous military and satellite applications, resulting in a power savings of 100:1, and a size reduction of 20:1 over bulk oscillators.⁹ SAW oscillators operate at fundamental frequencies beyond 1 GHz and have properties which effectively improve phase noise performance to the elimination of frequency multipliers and phase lock loop circuitry.

In controlling device characteristics such as temperature compensated frequency stability, high-Q and low phase noise, choice of substrate materials is an important decision in the design. To date, single crystal quartz is employed with several different crystal orientations applied. The lowest temperature coefficients have been achieved with the ST cut quartz. Since SAW resonators are presently fabricated on piezoelectric substrates, hybrid circuit technology must be employed to



MRDC41125.1FR

introduce the amplification feedback stage and buffer amplifier stage in the oscillator circuit.

Typically in this type of oscillator, the resonator is packaged separately from the oscillator circuitry, and a hybrid package is interfaced with the resonator. This approach has the disadvantage of wiring parasitics and a much larger resulting package. The approach under study in this program will eliminate the need for hybrid electronics since a monolithic single chip resonator/oscillator structure can be achieved. This report covers the results of such monolithic resonators using piezoelectric ZnO films on silicon. The high stability for the SAW oscillator with an aging rate of 10 ppm/year requires a systematic approach to resonator design as applied to thin film SAW resonators on silicon.

Two physical factors are also key in the design and fabrication of SAW resonators, dispersion and reflection in etched grating reflectors. Under this AFOSR contract, a new technique for the fabrication of resonator grooves using anisotropic etching has been developed. Reflection and transmission of this type of resonator structure were studied using multi-mode reflection techniques.² Micro structure definition of the etched wall reflectors was also studied using scanning electron micrography. Reflector fabrication with sub-micron geometry was demonstrated using the well-controlled anisotropic etching procedure. Such high definition results in not only uniform reflection characteristics, but also low



MRDC41125.1FR

dispersion, a key factor in extending the frequency range of SAW devices. Fabrication of resonator devices operating well into the GHz range should be possible using this anisotropic etching technique. A preliminary design of such a resonator is included in this report with center frequency above 400 MHz and a Q in the range of 25,000.

The ultimate objective of this research is to complete the integration of SAW devices and demonstrate integrated circuit oscillators on silicon in the GHz range. This approach would employ resonator structures as fabricated under this study integrated with FET or double-diffused MOS transistors on one chip. The condition of this phase of the study will determine the ultimate frequency limitations of integrated monolithic oscillators which eliminate many of the problems associated with wiring parasitics and package interfacing associated with present hybrid technology as applied to fundamental frequency oscillators in the microwave range.

2.1.2 THEORY OF OPERATION

The overall resonator performance is dependent on a number of design factors:

1. Piezoelectric material
2. IDT metal structure and thickness
3. IDT apodization
4. Reflector group depth
5. Reflector width

6. Reflector sidewall shapes
7. Reflector substrate material
8. Reflector microstructure

Many of the above factors are directly related to structures achievable in the reflector cavity which is strongly influenced by the choice of materials utilized. The silicon structures employed for reflector arrays in this study have had the advantage of wide process study and development associated with the integrated circuit industry. This, in addition to its higher inherent surface velocity, has allowed the achievement of acoustic properties in the reflector structure not previously possible with quartz or lithium niobate materials.

Reflector wavelength is chosen slightly smaller than transducer wavelength to compensate from the frequency shift resulting from the reduction of $\Delta v/v$ in the reflector structure. The depth of groove was chosen to minimize bulk losses in the reflector structure. Effective cavity length has been determined experimentally as a function of group depth to achieve an optimum number of reflector grooves within the cavity structure.

2.1.3 RESONATOR STRUCTURE

The surface acoustic wave resonator is a planar electrode structure photolithographically defined on a suitable piezoelectric material. The SAW resonator functions in much the same manner as a conventional quartz oscillator crystal.



MRDC41125.1FR

Acoustic waves are generated by an interdigital transducer which provides electrical-to-mechanical as well as mechanical-to-electrical signal transduction. The acoustic waves are confined within a cavity whose boundaries are accurately maintained. The Q of the cavity is determined by the material losses and cavity leakage. The same excellent frequency controlled properties of bulk wave quartz resonators is also achieved by SAW resonators provided that the fabrication techniques are closely controlled. Figure 1 is a schematic representation of three common types of resonator designs. The simplest type is that shown in part A of the figure, which is a single-pole, single-port resonator structure.

On either side of the input/output transducer are two gratings which contain a large number of reflecting structures with a periodicity slightly less than that in the transducer. The gratings act as mirrors when the acoustic wavelength is approximately equal to twice the grating periodicity. In this frequency range, all of the surface acoustic wave energy is confined within the cavity formed by the two gratings. Each grating acts like a mismatched impedance in the transmission line, causing a reflection. With a sufficient number of gratings, a total reflection from all the gratings can be achieved very nearly equal to the incident wave from the IDT transducer. At the resonance frequency, all of the reflections add in phase, resulting in a narrow band signal with extremely high Q factor.

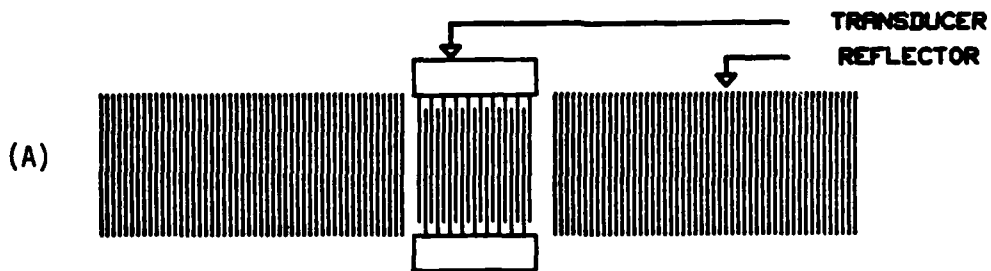
The one-pole, one-port resonator of Figure 1A has inherent low cross talk and lower insertion loss. The structure shown in Figures 1B and 1C have higher insertion loss due to propagation losses of an acoustic signal in the center of the cavity. However, these type of resonators have the advantage of a phase shift required for the construction of a positive feedback resonator controlled oscillator.

2.1.4 SILICON RESONATOR HIGH FREQUENCY ADVANTAGES

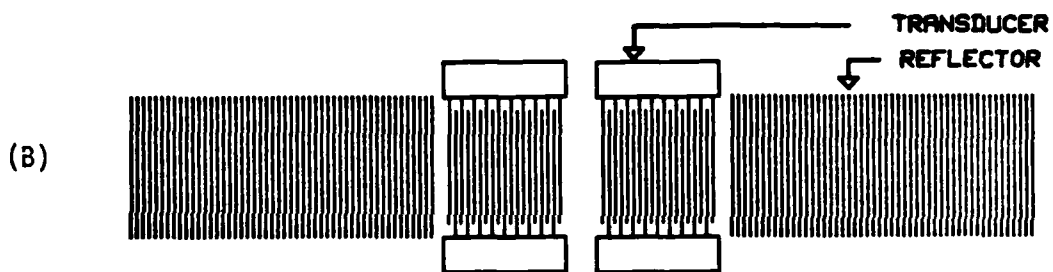
One of the key factors to consider in the performance of high frequency fundamental SAW resonators or SAW delay lines is the limitations of the state-of-the-art of present photolithography. The surface acoustic wave phase velocity on quartz is typically 3158 meters/second. At 1 GHz this results in a wavelength of 3.2 microns with lines and spaces 1/4 of that or 0.8 microns. At 1.6 GHz the line widths become even smaller since the wavelengths become 2 microns and the line widths approximately 0.5 microns. Since SAW structures have very high aspect ratio lines (very long lines with very narrow widths), they have significantly more stringent photolithography requirements than conventional integrated circuits. For example, a 1 GHz SAW resonator may have a typical line length of over 1000 microns while having a line width of 0.8 microns, resulting in an aspect ratio of over 600:1. A critical design requirement for uniform surface wave frequency generation is that all line widths and spaces be uniform over the entire length of the IDT, as well as



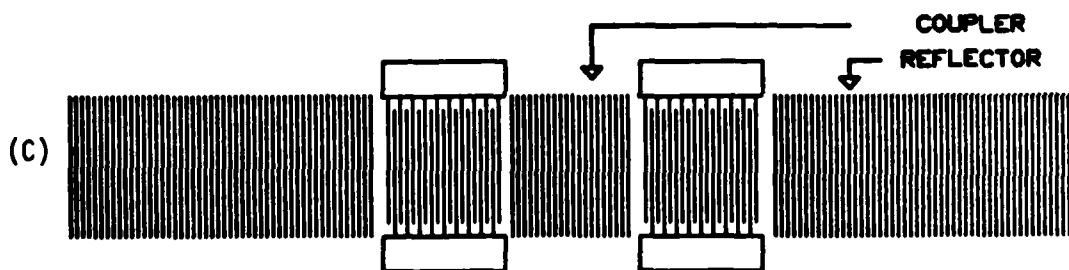
MRDC41125.1FR



SAW SINGLE PORT RESONATOR



SAW 1 POLE 2 PORT RESONATOR



SAW 2 POLE 2 PORT RESONATOR

Fig. 1 Saw resonator cavity structures.

in the reflector structures. Therefore, the processing must be controlled so that line widths and spaces are uniform from line to line and from device to device.

In comparing silicon with common piezoelectric substrate materials, silicon is found to have a significant velocity advantage. A comparison of acoustic velocities for common piezoelectric and semiconductor materials is given below:

MATERIAL	ACOUSTIC VELOCITY
Quartz	3158 m/sec
LiNbO ₃	3472 m/sec
GaAs	2763 m/sec
ZnO/SiO ₂ /Si	4076 m/sec
Silicon	4921 m/sec

Naturally, a material with a higher acoustic velocity will produce a higher frequency resonator or oscillator for an equivalent grating spacing. Figure 2 is a plot of device frequency as a function of line spacing for the above-mentioned materials.

2.1.5 DEVICE MODELING

As with other electronic devices, theoretical modeling gives a more detailed insight and understanding of resonator device operation prior to determining final design.

The resonator cavity consists of two distributed reflectors spaced symmetrically on either side of the input/output transducers. Several key parameters directly affect or relate to



MRDC41125.1FR

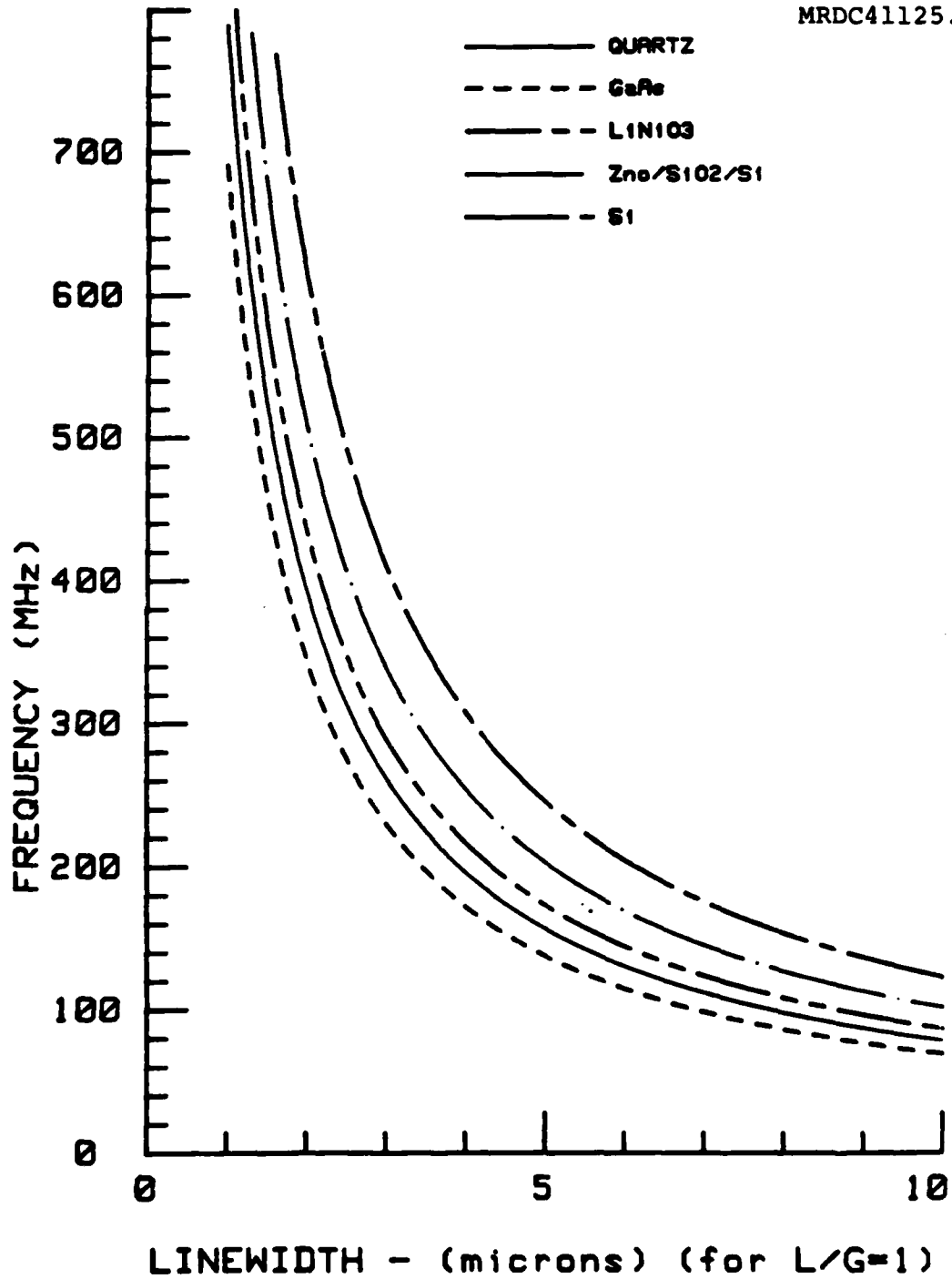


Fig. 2 Device frequency as a function of linewidth for different substrates.



the performance of the resonator, as shown in Figure 3, and as listed below:

- ϕ_r : acoustic reflection factor
- d : gap spacing from IDT to reflector
- N_{gt} : IDS spacing in half wavelengths
- N_{gr} : reflector spacing in half wavelengths
- N_x : effective reflector penetration distance in half wavelengths
- L_{eff} : effective cavity length

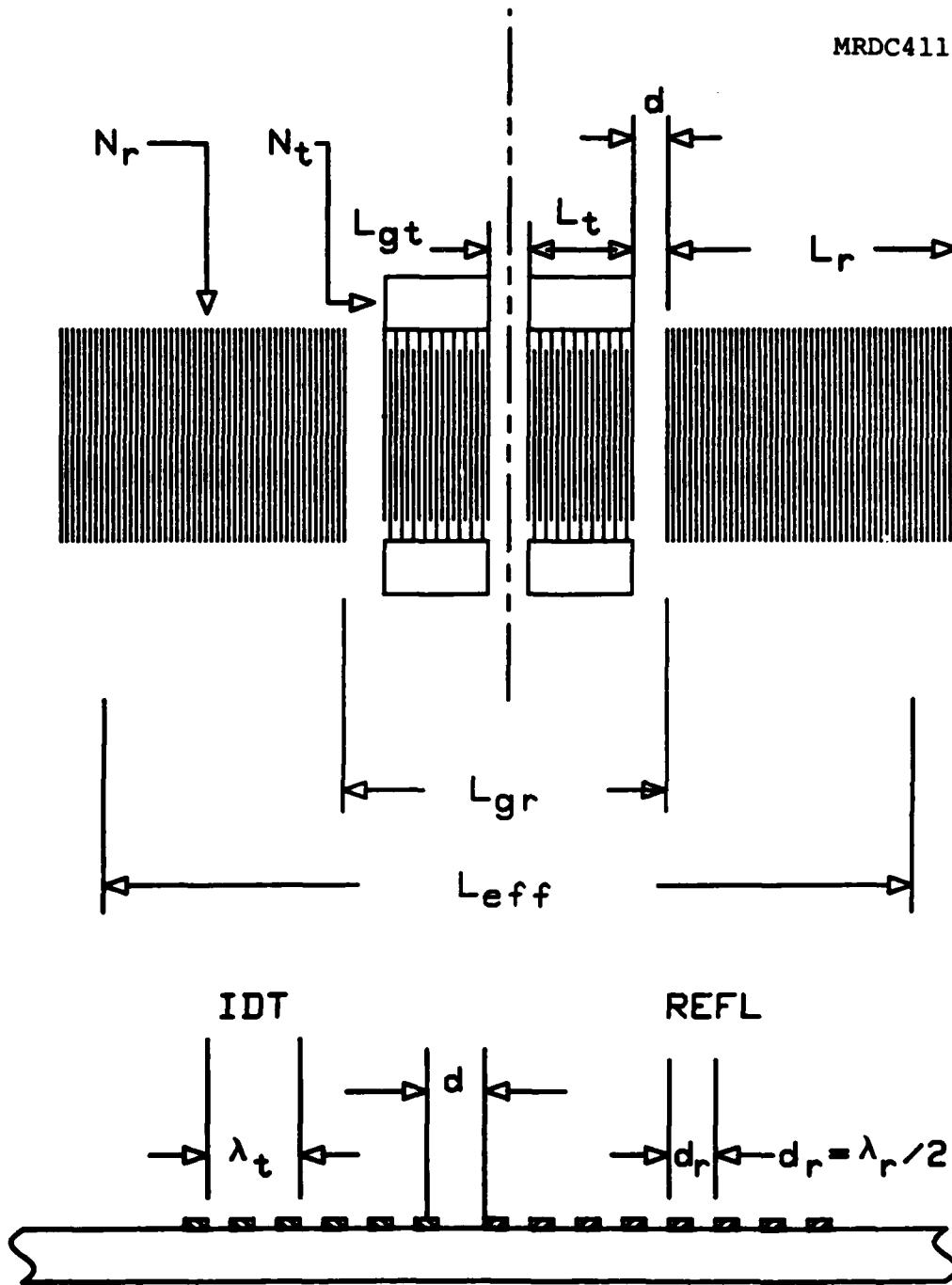
All of these parameters (except N_{gr} and L_{eff}) can be determined by the reflector properties if the groove shapes are precisely known. To determine values of N_{gr} and L_{eff} the exact value of SAW velocity must be measured. Fortunately, since this data is not available in the initial design phase, it is necessary to first design and test a preliminary resonator structure several frequencies above and below resonance utilizing the same reflector. In this way, measurements can be made on the test structure to precisely determine SAW velocity.

Many properties can be determined with the experimental measurements of multi-mode resonators. Typical narrow gap resonators with a high Q have only one mode of resonance and contain relatively little information about reflector properties.

2.1.6 SINGLE MODE RESONATOR

Total reflection from within the resonator cavity can be determined by considering impedance mismatched perturbation due to each reflector grating. If Z and Z' are transmission line

MRDC41125.1FR



2 PORT RESONATOR DETAIL

Fig. 3 General resonator structure and key parameters for design.



MRDC41125.1FR

The magnitude of the reflection, $|R|$, at the center frequency and the condition that $|\epsilon| \ll 1$ can be expressed as

$$|R| = \left(1 - \frac{\alpha}{\epsilon'}\right) \tanh(N_r \epsilon') \quad (4)$$

where

$$\epsilon' = |\epsilon \sin(\pi \ell)| \quad (5)$$

From equation (4), it is clear that,

$$|R|_{(max)} = \left(1 - \frac{\alpha}{\epsilon'}\right) \quad (6)$$

The quality factor, Q , for the resonator is defined,

$$Q = \frac{2\pi L_{eff}}{1 - |R|^2} \quad (7)$$

using relation (6) we get

$$Q_{(max)} = \frac{\pi L_{eff} \epsilon'}{\alpha} \quad (8)$$

Assuming $\delta = 0.2$ and loss less reflectors, reflection phase, ϕ_R can be expressed as

$$\phi_R \approx -\tan^{-1} \left[\frac{\delta}{1 + \frac{S_{n-1}(P)}{S_n(P)}} \right] \quad \epsilon > 0 \quad (9)$$

$$\phi_R \approx -\tan^{-1} \left[\frac{\delta}{1 + \frac{S_{n-1}(P)}{S_n(P)}} \right] + \pi \quad \epsilon < 0$$



MRDC41125.1FR

impedances for the gap area and for the reflector area respectively, then we define ϵ as a relative mismatch coefficient.

$$\epsilon = \frac{Z}{Z'} - 1 \quad (1)$$

If we set Z equal to Z/Z' (impedance ratio of reflector to gap) then

$$\epsilon = z - 1 \quad (2)$$

We can define parameter γ as a complex phase shift per reflector section,

$$\gamma = (\pi + \delta) - i\alpha \quad (3)$$

where δ is a function of center frequency deviation. Both δ and γ should be determined experimentally for any SAW resonator cavity structure. For an ideal resonator at resonant frequency (f_r) the value of $\delta = 0$. In most practical devices, $\delta = 0.2$ is acceptable.

α (attenuation constant) is a measure of losses in the substrate material employed. Although α is not usually equal to zero, propagation losses in many materials are relatively small, in the range of a few hundredths of a dB/cm.



where

$$P = [|\epsilon'^2 - \delta^2|]^{1/2} \quad \text{and} \quad n = N_r \quad (10)$$

The functions S_n are derived from Chebyshev polynomials of the second kind of order n

$$\begin{aligned} S_n &= (-1)^n \sinh(np) & \epsilon' > |\delta| \\ S_n &= (-1)^n \sin(np) & \epsilon' < |\delta| \end{aligned} \quad (11)$$

To find the optimum value of d for our cross-field IDTs, when $\epsilon > 0$ (corresponding to zero reflection phase at the center frequency) then d should be tuned to a length equal to an integer number of $\lambda/2$. If $\epsilon < 0$, however, at center frequency, the phase reflection is 180° and consequently d will be optimized at a length shifted about a quarter of acoustic wavelength. Therefore,

$$\begin{aligned} d_{opt} &= m \frac{\lambda}{2} & \epsilon > 0 \\ d_{opt} &= (m - 1/2) \frac{\lambda}{2} & \epsilon < 0 \end{aligned} \quad (12)$$

ϵ , α and L_{eff} are the important parameters to be determined in order. ϵ is determined from measuring acoustic coupling. To find α , normalized Q of the resonator can be plotted as a function of reflector numbers, N_r , experimentally and then curve fitted to the theoretical values with α being a parameter. Normalized Q can be determined from equations (6) through (8).



MRDC41125.1FR

$$\bar{Q} = \frac{Q}{Q_{max}} = \left[1 + (2\epsilon'/\alpha)e^{-2N_r\epsilon'} \right]^{-1} \quad (13)$$

Since ϵ' is now determined, \bar{Q} can be numerically plotted as a set of α curves, each as a function of the number of reflectors, N_r . From the normalized Q plot, effective cavity length and L_{eff} can be determined using the saturation point.

Since one key aspect of the program is to evaluate anisotropically-etched reflector structures with sloped sidewalls in silicon, the multi-mode resonance method is again useful. As the cavity length increases, the number of excited modes increases and the difference frequency between modes is measured. Assuming negligible reflection contributed from the IDT, the difference between mode frequencies remains constant (f_m). From f_m , L_{eff} is determined. Referring to Figure 3,

$$L_{eff} = L_{gr} + 2 L_x$$

where L_{gr} is the distance between the inner edges of the reflector and L_x is the effective penetration distance to the reflector. If f_r is the cavity resonance frequency, and acoustic wavelength is λ_r , then we have

$$N_x = \frac{1}{2} [f_r/f_m - N_{gr}] \quad (14)$$

where N_x and N_{gr} defined in Figure 3. From equation 14 the effective cavity length can be derived:



MRDC41125.1FR

$$L_{eff} = (N_{gr} + 2N_x)\lambda_r/2 \quad (15)$$

From equation (15) we can write

$$\epsilon = \frac{1}{2}N_x \quad (16)$$

since,

$$f_m = \frac{v}{2(L_{gr} + 2L_x)} \quad (17)$$

and

$$N_x = \frac{1}{2n} \left(\frac{d\phi R}{d(f/f_r)} \right) \quad (18)$$

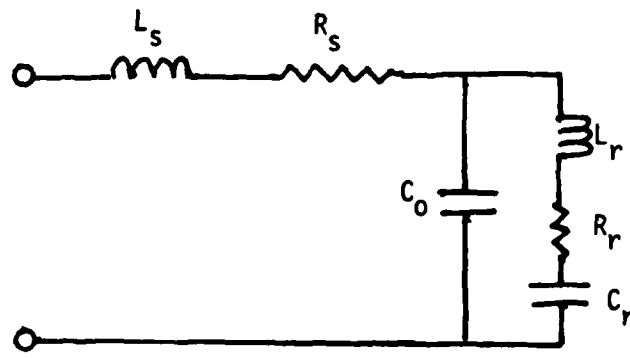
$\frac{d\phi R}{df}$, phase slope can be determined from equation (18).

$$\frac{d\phi R}{df} = \frac{2\pi N_x}{f_r} \quad (19)$$

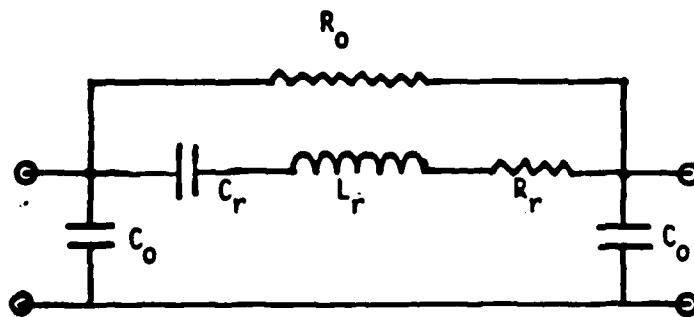
2.1.7 EQUIVALENT CIRCUIT MODELS

Equivalent circuits for both one-port and two-port resonators are shown in Figure 4. Elements of both circuits are quite similar with C_r , L_r , and R_r as resonant elements. C_o is the static capacitance of the IDT where R_g and L_g are the parasitic resistance and parasitic conductances, respectively. More details of this work, related to characterization of ZnO delay lines are reported previously.¹⁰

MRDC41125.1FR



(a)



(b)

Fig. 4 (a) Equivalent circuit for one-port resonator;
 (b) equivalent circuit for two-port resonator.



MRDC41125.1FR

Since the multi-mode resonator is the basic structure under study in this program, we will discuss this structure in the one-port resonator configuration in more detail.

The static capacitance, C_0 , and the resonant elements R_r , L_r , and C_r will be determined using the physical parameters and material properties shown in Table 1.

C_0 can be expressed

$$C_0 = \frac{N_t \epsilon_t W_t \lambda_t}{8h} \quad (20)$$

where N_t , ϵ_t , W_t , λ_t , and h are defined in Table 1. R_r is the real value in the resonant equivalent circuit and can be expressed as

$$R_r = \frac{1 - |R|}{G_0(1 + |R|)} \quad (21)$$

where

$$G_0 = 8K_p f_t C_0 N_t \quad (22)$$

and the case of K_p , f_t and N are defined in Table 1. $|R|$ has been given previously in equation 4. L_r and C_r are the reactive elements of the resonant circuit and are expressed as follows:

$$L_r = \frac{L_{eff} \lambda_r}{G_0 f_r (1 + |R|^2)} \quad (23)$$

$$C_r = \frac{G_0 (1 + |R|^2)}{4\pi^2 \lambda_r f_r L_{eff}} \quad (24)$$



TABLE 1

PARAMETER	DESCRIPTION	UNIT
ϵ_t	Dielectric Constant	$10\epsilon_0$
h	Thickness of ZnO	Microns
ϵ	Relative Mismatched Impedance	Numbers
α	Attenuation Constant	Cm^{-1}
N_r	Number of Reflector Elements	Numbers
N_t	Number of Transducer Fingers	Numbers
Q	Quality Factor of Resonator	Numbers
R	Reflection Coefficient	Numbers
λ_t	IDT Wavelength	Microns
λ_r	Reflector Wavelength	Microns
f_t	IDT Center Frequency	MHz
f_r	Resonance Frequency	MHz
L_x	Penetration Depth in Reflector	Mils
Lg_r	Length of Reflector Gap	Mils
Lg_t	Length of Transducer Gap	Mils
N_x	Penetration Depth in Unit $\lambda_r/2$	Numbers
L_r	Length of the Reflectors	Mils
L_t	Length of Transducer	Mils
f_m	Mode frequency	MHz
W_t	Length of Transducer Electrodes	Mils
W_r	Length of Reflector Electrodes	Mils

where λ_r and f_r are defined in Table 1. L_{eff} has previously been given by Equation 15.

The amplitude and phase response of a typical 355 resonator are shown in Figure 5, as derived from the equivalent circuit model.

2.1.8 FREQUENCY STABILITY

Frequency stability for a high accuracy, high-Q elect oscillator is determined by the stability of the crystal, in case a thin film SAW resonator. For SAW devices on piezoelectric substrates, the stability is controlled by temperature coefficient of delay (TCD) of the surface wave the substrate. The temperature coefficient of delay depends only on the type of substrate material, but the orientation the crystal cut employed in fabricating the device. The T the material affects the phase velocity of the surface wave therefore the wavelength and frequency of oscillation. silicon SAW resonators the phase velocity of surface wave controlled by the combined effects of temperature variations the silicon substrate as well as in the SiO_2 and ZnO thin films that are employed.

By controlling the thickness of the SiO_2 thermal oxide the ZnO thin films to appropriate values, a near zero temperature coefficient of delay can be realized. For characterization modeling of the resonator during this phase of the study previously reported technique for characterization of delay



MRDC41125.1FR

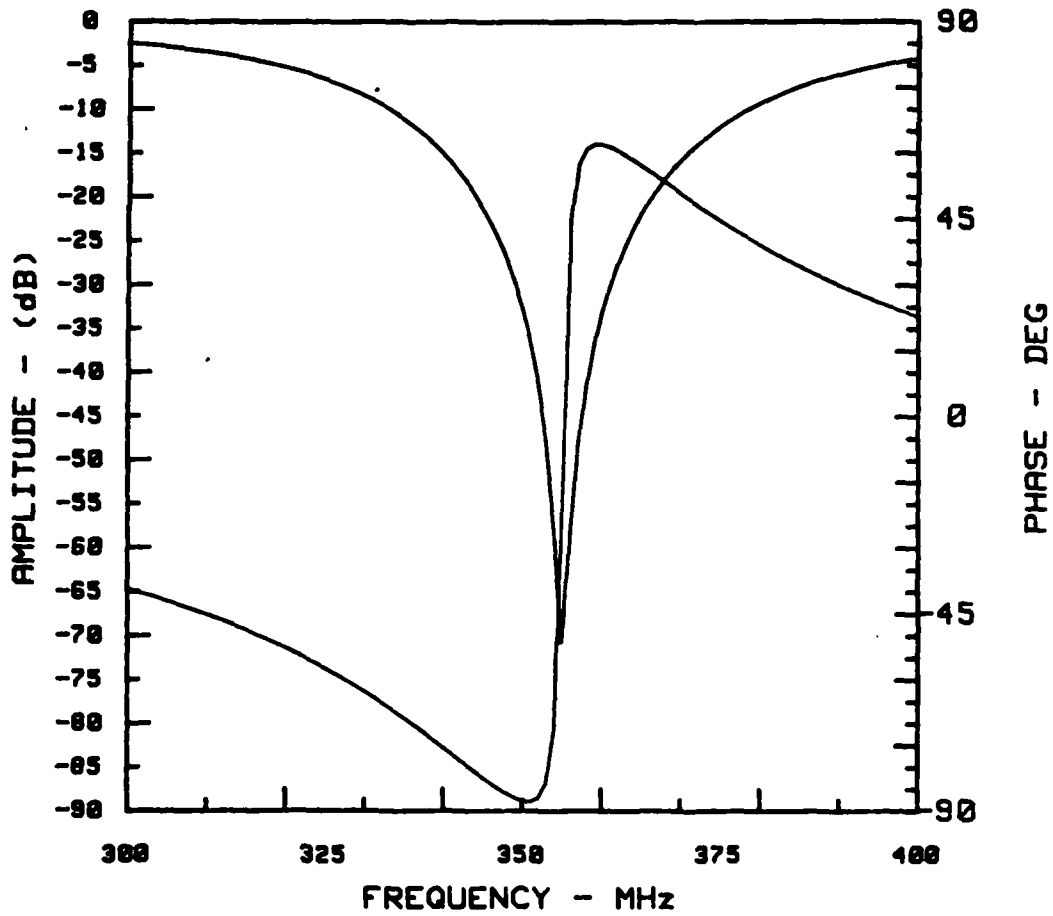


Fig. 5 Amplitude and phase responses of a 355 MHz saw resonator driven from the equivalent circuit model.



MRDC41125.1FR

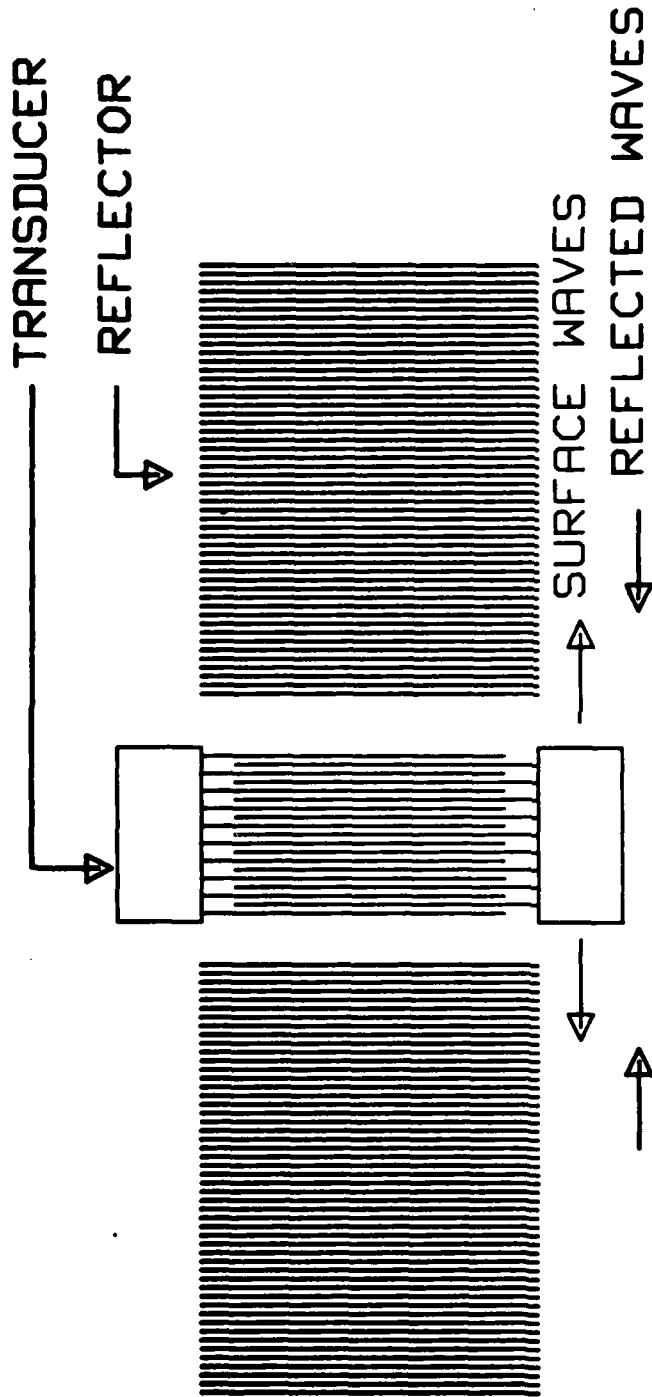
in resonators was used. In this approach, both impedance properties and stability are measured and compared with theoretical models using a system of measurement hardware and computational software. The measurement system contains considerable hardware in the form of phased locked network analyzers, spectrum analyzers and stability analyzers. All of the system is interconnected and controlled from a dedicated computer. The computer is able to control and take measurements as well as analyze the results in terms of models based on the physics and chemistry of the device.

2.2 DEVICE DESIGN

Since the initial phase of the program was to demonstrate feasibility and characterize SAW thin film resonators on silicon, initial designs centered on a device with an apodized interdigitated transducer (IDT) coupled to a multi-mode resonator cavity. The multi-mode cavity has larger-than-normal gap spaces between the IDT and resonator structures so that several reflection modes may be studied to determine resonator cavity characteristics. Frequency range of the reflecting modes varied from 330 MHz to 370 MHz. Many devices were fabricated and characterized, the results of which are presented later in this report.

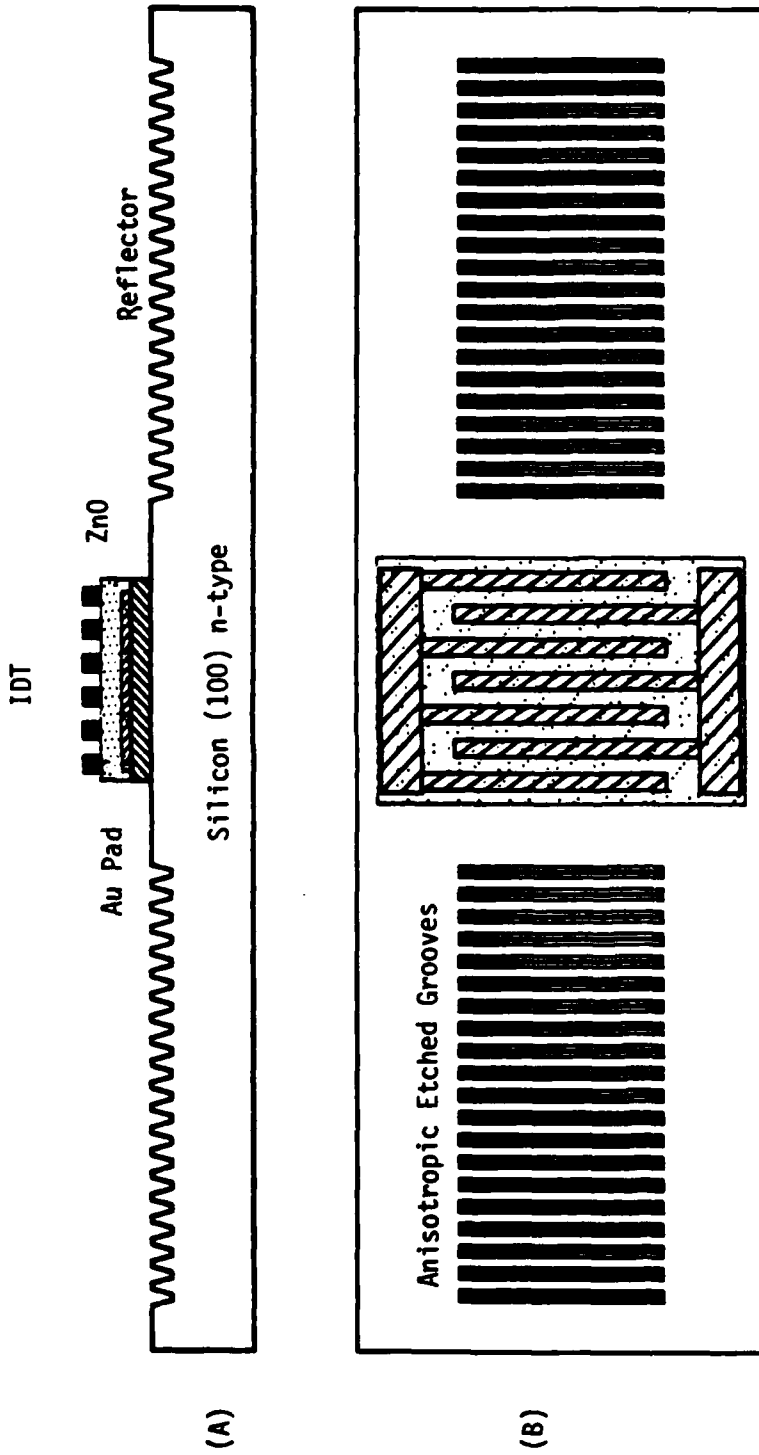
2.3 MASK DESIGN AND FABRICATION

A general the single-pole, one-port multi-mode resonator structure is shown in Figure 6. Figure 7 shows a cross-sectional



SAW SINGLE PORT RESONATOR

Fig. 6 Saw one-port multi-mode resonator structure.



SAW ZnO/Silicon RESONATOR

Fig. 7 Cross-sectional view of a one-port resonator after processing.



MRDC41125.1FR

view of a device after fabrication. The substrate is a silicon (100) orientation and the device is fabricated parallel to the (110) flat location on the silicon substrate.

The first mask is used for growing a 1 micron thermal oxide to pattern the reflector opening. The silicon dioxide acts as a masking material for anisotropic etching. After the etching process is completed, the SiO_2 is removed and a second thermal oxide (7000-9000 angstroms) is grown.

A thin layer of gold is then deposited to act as a field plate under the IDT area (see Figure 7). Next, a 3300 angstrom film of ZnO is sputter deposited. Using appropriate resist technology, the excess ZnO is removed by a wet chemical etch, which is followed by a dry etch for removal of unwanted SiO_2 . Then a 2000 angstrom layer of aluminum is deposited, using E-beam vacuum evaporation. The aluminum film is then patterned to form the IDT electrode structures.

Only four masks are necessary to process the entire device. Figure 8 is a computer scaled plot superimposing all of the four mask layers. Figure 9 shows the IDT mask detail with cosine-hyperbolic-cosine weighting in the electrode structure. The IDT has an acoustic beam width of 75 wavelength and utilizes 40 finger pairs.

2.4 RESONATOR FABRICATION

As outlined in previous sections, the anisotropically etched resonator structures are produced using a wet etch process of

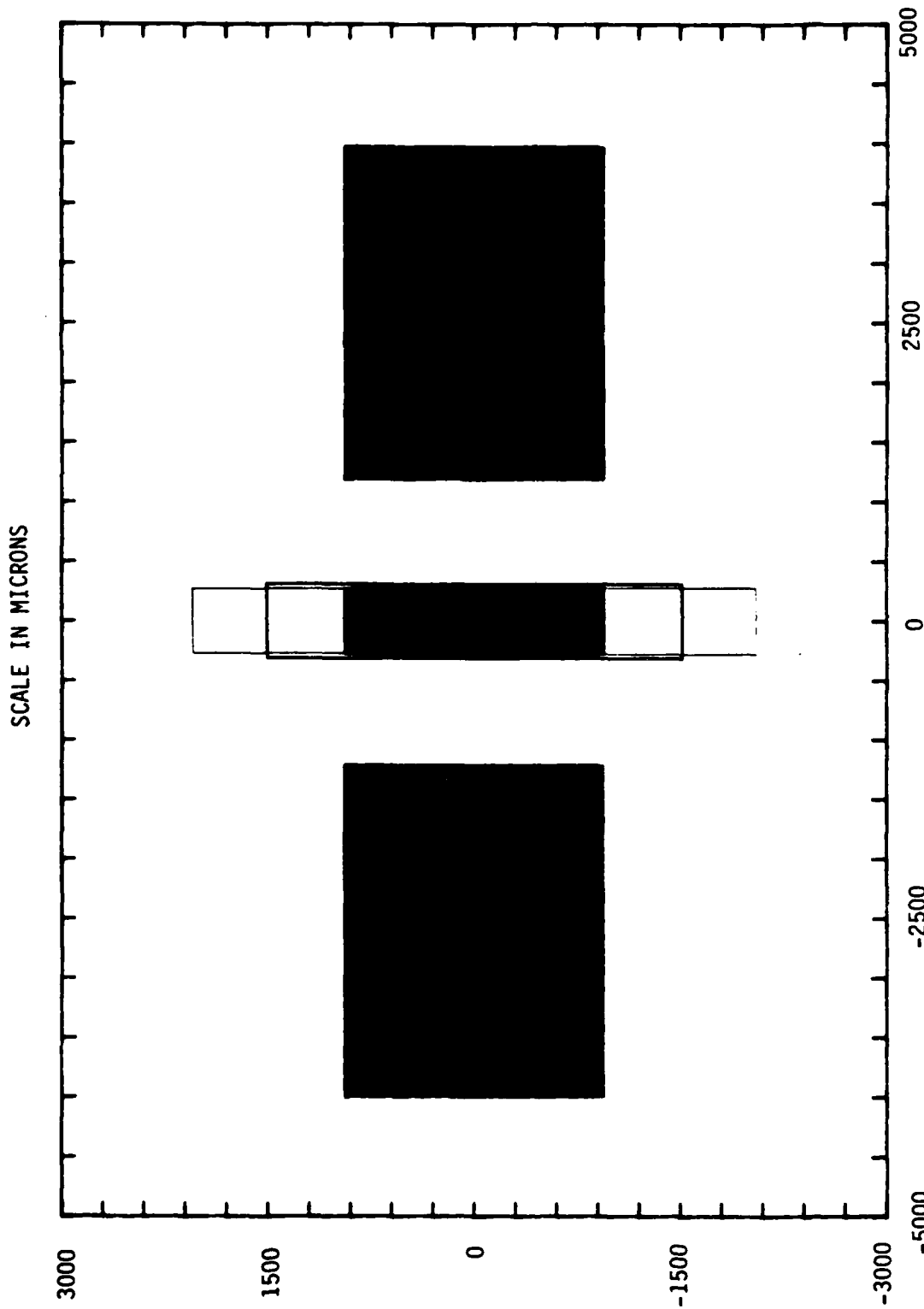


Fig. 8 Computer plot of actual design superimposing all of the four mask layers.



MRDC41125.1FR

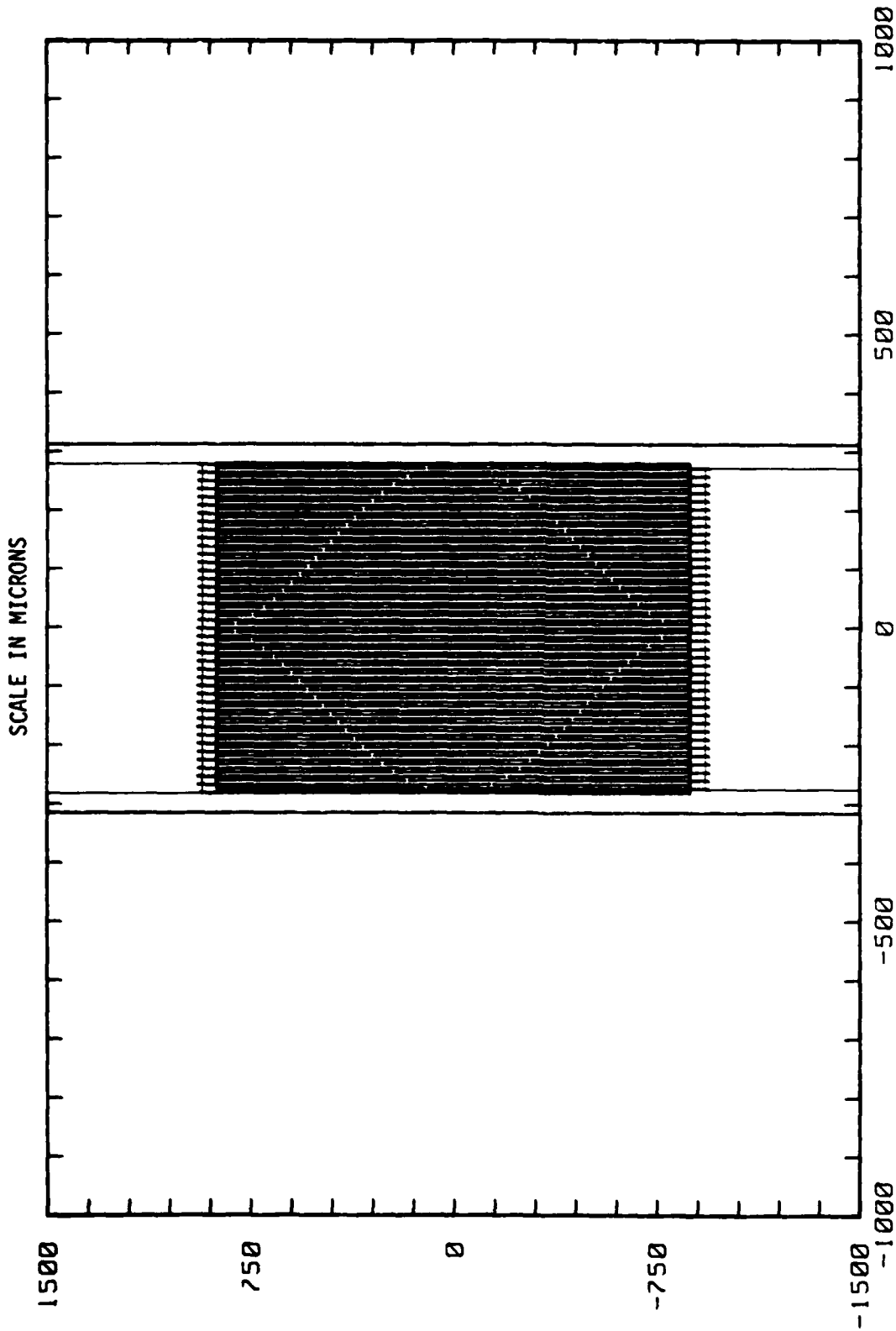


Fig. 9 IDT mask detail with cosine-hyperbolic-cosine weighting in the electrode structure.



MRDC41125.1FR

ethylene diamine and pyracatachol, commonly referred to as EDP. Fabrication of microstructures anisotropic etching of Si is influenced by the following factors:

1. The crystallography perfection of the substrate;
2. The geometry of the surface pattern delineated on an appropriate masking film on the substrate surface;
3. Control of anisotropic etching conditions.

Thermally grown silicon dioxide has been demonstrated to be an excellent masking for EDP and is part of our MOS processing. EDP etching is performed in a specially designed chamber where temperature and circulation are carefully controlled. The etch rate is approximately 1 micron/min for (100 oriented) surfaces. Only 40-50 seconds are required for complete reflector fabricaton. While other etch methods were evaluated, the best results were obtained using EDP. SEM studies showed better etching control and superior sidewall definition using EDP as compared to other wet etching techniques or reactive ion etching approaches (RIE).

Figures 10 and 11 are SEM photographs taken from a silicon resonator groove fabricated by EDP etching. The figures demonstrate the excellent sidewall definition and control of center-to-center spacing of reflectors.

Temperature coefficient of delay for layers of ZnO and SiO₂ on silicon substrates has theoretically and experimentally been determined. It has been demonstrated that controlling the



MRDC84-26676

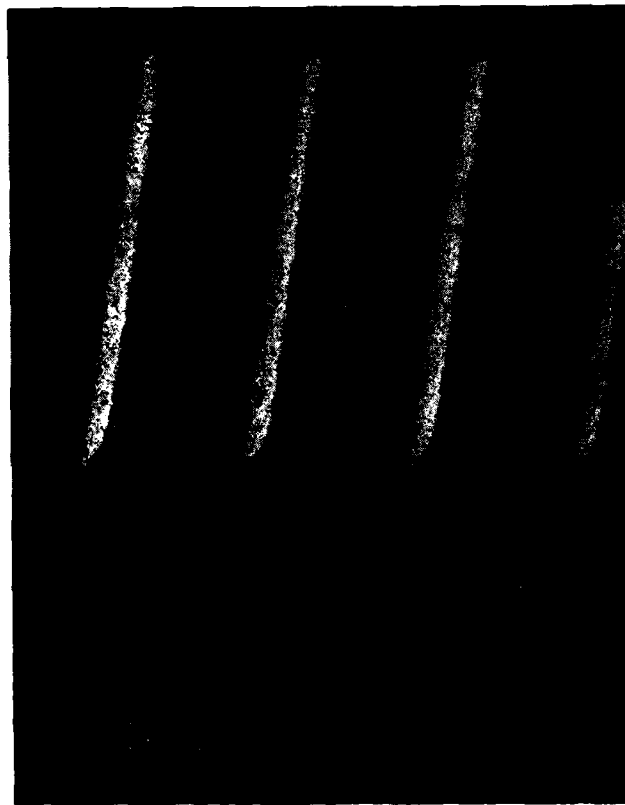


Fig. 10 SEM picture of a silicon resonator groove using anisotropic etching technique.



MRDC84-26677

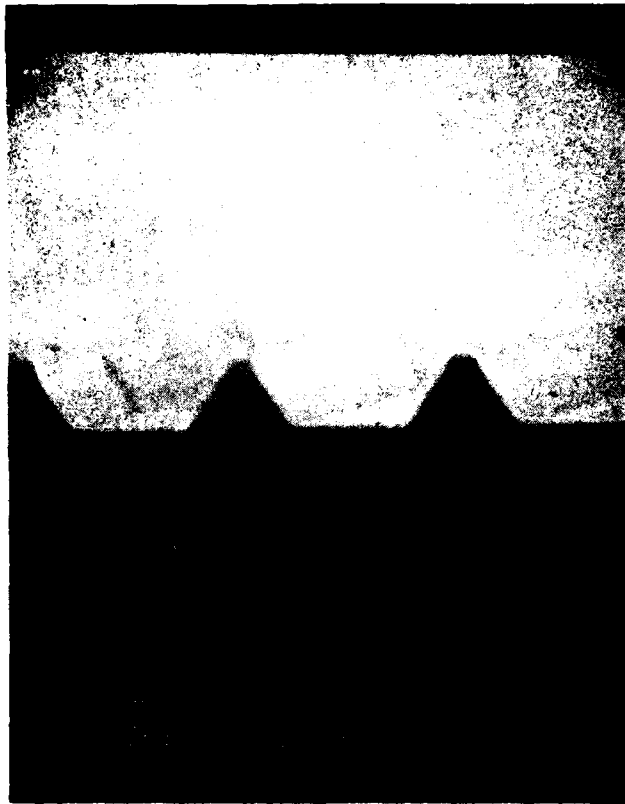


Fig. 11 SEM picture of a reflector cross section using anisotropic etching technique.



MRDC41125.1FR

thickness of these layers to appropriate values will result in a zero temperature coefficient of delay over a temperature range of 0-100°C. Normalized to the surface acoustic wavelength, the ZnO thickness should be 0.032 microns and the SiO₂ thickness should be 0.076 microns.

2.5 EXPERIMENTAL RESULTS

After wafer processing is completed, the resonators are separated using conventional silicon sawing and dicing methods. Figure 12 shows one-half of a 3" silicon wafer containing twenty-six, 355 MHz single-pole multi-mode cavity resonators. After dicing, each resonator is mounted in a hermetically sealed TO8 package. One device mounted in such a package can be seen in Figure 12, with the cover of the package at the left. The devices are then tested and characterized using a 50 ohm impedance matched fixture. A photograph of the test fixture is shown in Figure 13.

Several lots of wafers were processed and completely characterized. The first lot was designed to a center frequency of 355 MHz. Other lots were designed to a center frequency about 5% on either side of the center frequency.

The S11 amplitude response (return loss) for a single-pole multi-mode resonator is shown in Figure 14. The sharp resonance of each of the modes is indicative of well defined sidewall surfaces of the reflectors. Using the equations derived in



MRDC84-26678

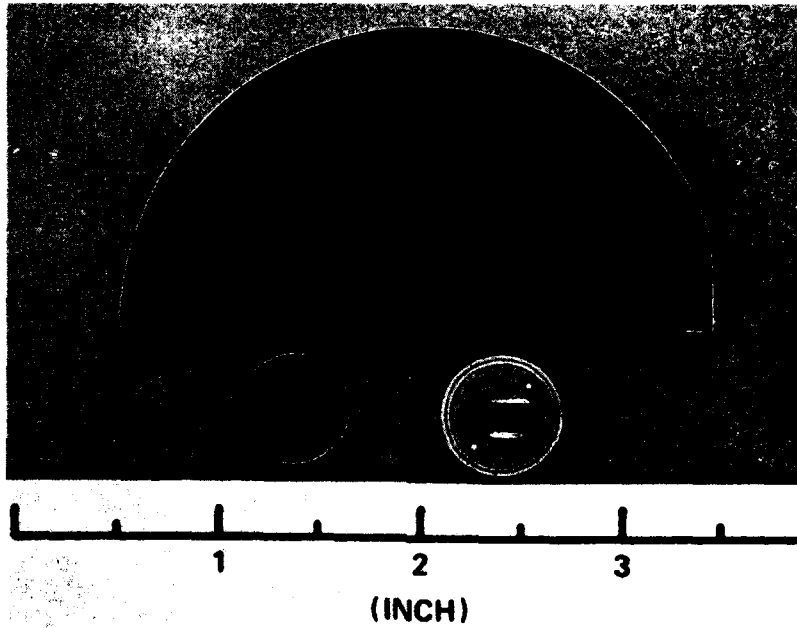


Fig. 12 A portion of a 3-inch silicon wafer containing 26 resonators with one device mounted in TO-8 package.



MRDC84-26679

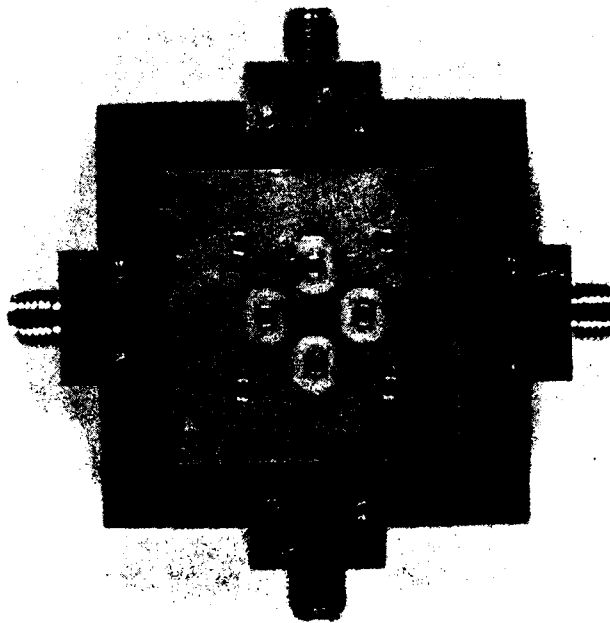


Fig. 13 50-OHM matched fixture is designed for resonator characterization after mounted in TO-8 package.

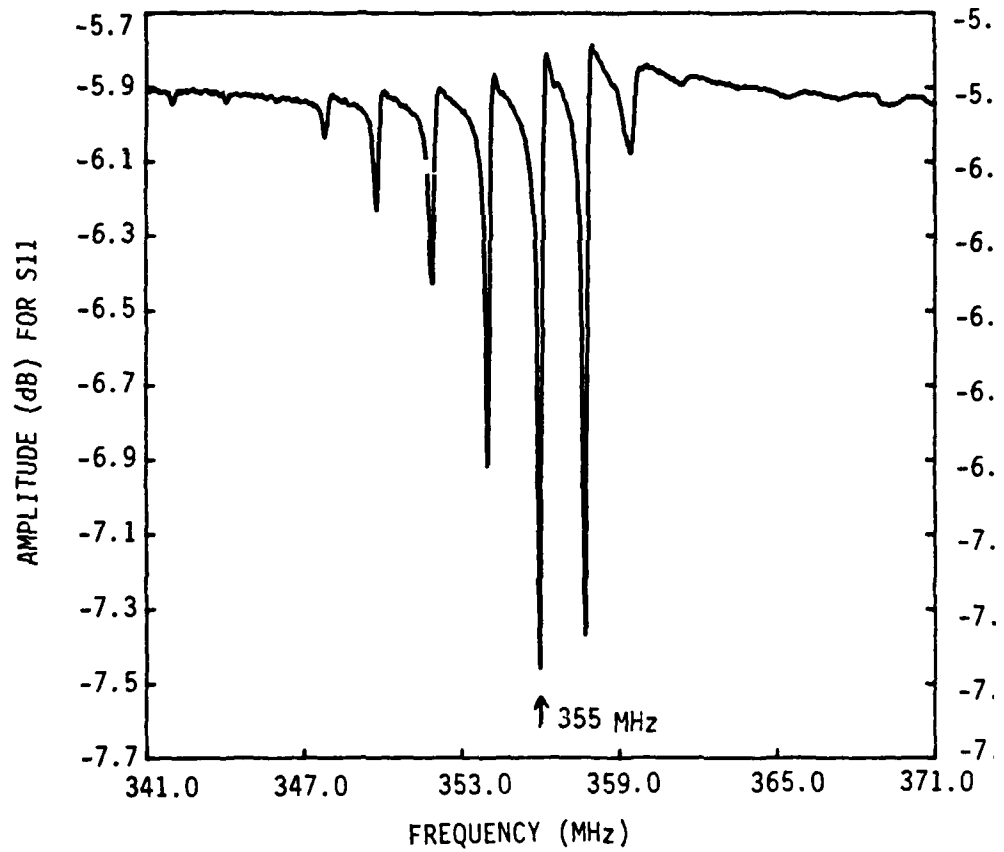


Fig. 14 Experimental plot of return loss amplitude for resonator with a wide gap. Several modes of res including 355 MHz mode are shown.

MRDC41125.1FR

Section 2.2, the key resonator characteristics have been determined.

Using Equation 15, we have

$$L_{eff} = (N_{gr} + 2N_x) \frac{\lambda_r}{2}$$

where $N_{gr} = 192$ from design and $\lambda_r = 12.5$ microns, then

$$N_x = \frac{1}{2} [f_r / f_m - N_{gr}] \quad (25)$$

f_r and f_m are defined in Section 2.2. From those definitions, we have $f_r = 355$ MHz and $f_m = 0.494$ MHz, where f_m is the mode frequency and is measured by averaging several data responses of multi-mode resonances. Using the above equations, we can determine

$$N_x = 263$$

N_x is the effect of penetration distance of the reflector in units of $\lambda_r/2$. Using the value of N_x , the effective cavity length is

$$L_{eff} \text{ approximately} = 4.572 \text{ mm (180 mils).}$$

Having determined penetration distance N_x , we have

$$\epsilon = \frac{1}{2N_x} = 0.002$$

using Equation 19, the phase slope can be determined

$$\frac{d\phi R}{df} = \frac{2\pi N_x}{f_r} = 4.67 \times 10^{-6} \quad (26)$$



MRDC41125.1FR

For a high-Q resonator with a single IDT, the length of L_{gr} should be reduced to a value very close to L_t , where L_{gr} is the total reflector gap including L_t , the IDT length.

From the above evaluation of effective penetration distance and other parameters, it can be shown that 440 reflectors on each side of the cavity are necessary to maximize the Q of the resonator.

3.0 CONCLUSION

The objectives of the surface acoustic resonator on silicon study program were successfully completed. A multi-mode SAW resonator using thin film ZnO on silicon was designed, fabricated, and characterized. Methods were developed for effectively processing reflector structures in silicon using anisotropic etching. It was concluded that anisotropic etching methods results in well-defined sidewall structures for reflector cavity elements, producing a superior resonant cavity performance with lower phase noise than conventional quartz or lithium niobate structures. The data obtained from the thin film ZnO resonator structure on silicon has confirmed the feasibility of fabricating integrated SAW oscillators on a single monolithic chip. During this first year study phase of the program, Rockwell was able to successfully achieve its objectives and demonstrate device feasibility. Moreover, highly promising performance of future device designs is predicted based on the results achieved. Ethylene diamine pyrocatachol (EDP) chemical etching with thermal oxide masking was demonstrated as an excellent method for cell reflector fabrication. Sidewall definitions were far superior to those obtained by other methods and suggest capability of very high frequency performance which should be studied in the future. Three different resonator designs were evaluated with varying center frequencies to evaluate device performance. Thin film ZnO piezoelectric

MRDC41125.1FR

transducers were developed with high coupling factor for generation and detection of surface acoustic wave signals. A silicon dioxide isolation platform was successfully used for isolation of the thin film IDT structure from the effects of the silicon substrate. The resonator devices were mounted in T08 packages and tested with impedance matched 50 ohm fixtures.

Automated measuring equipment was employed to evaluate devices and confirm equivalent circuit models. Device performance very closely matched original circuit models showing excellent confirmation of design parameters.

A complete characterization data set was obtained from several lots of silicon wafers in the frequency ranges from 330 - 370 MHz. The results of this data indicated an effective cavity length of 4.57 mm (180 mils) for 355 MHz devices. Relative impedance mismatch near absolute value of epsilon was determined to be 2×10^{-3} demonstrating a phase slope of 4.6×10^{-6} . The effective cavity length was determined showing 440 reflectors in each cavity are required for maximizing the quality factor of the devices. The following section details plans for future studies to further determine high frequency limitations of these materials for the revolutionary thin film SAW devices on silicon capable of full monolithic integration. The importance of these results cannot be underestimated.



4.0 RECOMMENDATIONS FOR FUTURE EFFORT

Rockwell has been greatly encouraged by the results of this program. All of the preliminary goals were demonstrated and results achieved on high definition reflector structures show very promising performance for very high frequency thin film surface acoustic wave resonators and oscillators on silicon. The initial structures were evaluated in the 350 MHz frequency region. We feel it is of paramount importance to conduct further studies to determine the ultimate high frequency limitations using reflector structures with such high definition as those obtained using the EDP etching techniques. Proposed areas of investigation are:

TASK 1--Experimental Study of High Frequency Limitations of Piezoelectric Films Applied for SAW Resonators

1. Piezoelectric films surface topology
2. Piezoelectric coupling coefficient
3. Reflection and dispersion coefficients
4. Bulk effect resulting of groove depth
5. Effective cavity length
6. Maximum available Q
7. Temperature stability limitation
8. Process limitation in IDT and reflectors

TASK 2--Theoretical Modeling for Shaped Reflectors

1. Theory of acoustic scattering of sloped grooves
2. Electrical excitation of piezoelectric resonators



3. Multimode resonance theory
4. Stored energy and power loss mechanism
5. Resonator equivalent circuits
6. Derivation of equivalent circuit elements

TASK 3--Experimental Methods for Material Characterization

1. Material selection criteria
2. Processing methods
3. Multimode resonance analysis
4. Characterization and testing

Resonator structures well beyond 1 GHz perhaps as high as 4-5 GHz may well be possible. Sub-micron lithography techniques in conjunction with high resolution high frequency resonator structures should be studied to determine the ultimate limitations of this approach.

Other areas requiring a more thorough evaluation for this approach are:

1. Crystal structure and orientation as well as surface topology of piezoelectric thin films;
2. A thorough evaluation of piezoelectric coupling, reflection and dispersion coefficients;
3. Bulk effects due to reflector groove depth;
4. High frequency limitations of temperature stability characteristics.



MRDC41125.1FR

The thin film candidate materials for the next phase of this study are ZnO and AlN (aluminum nitride). Also, high frequency limitations of transistor amplifier structures in silicon and in other materials should be evaluated for integration with the resonator structures to achieve highly stable integrated monolithic thin film SAW oscillators. The process developed under this study is completely compatible with CMOS or DMOS FET processing. The feasibility of a monolithic crystal controlled oscillator should be carried to a logical conclusion. Figure 15 outlines the approach for the completely integrated silicon SAW oscillator.



MRDC41125.1FR

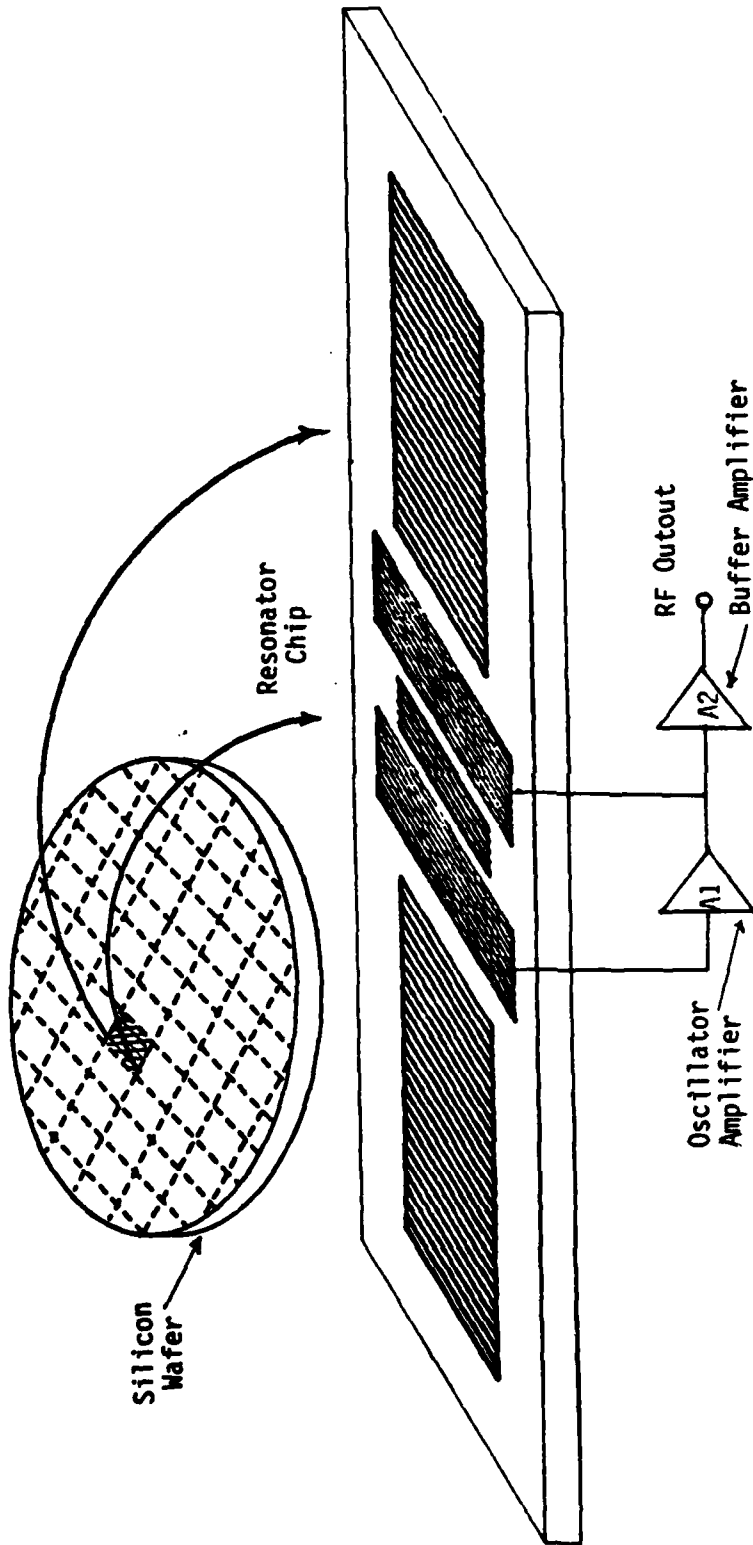


Fig. 15 Monolithic saw oscillator on silicon wafer showing the complete integration.



5.0 REFERENCES

1. E. A. Ash, "Surface Wave Grating Reflectors and Resonators," IEEE Symposium Microwave Theory and Techniques, held in Newport Beach, CA, May 11-14, 1970.
2. W. H. Haydle, B. Dischler and P. Heisinger, "Multimode SAW Resonator--A Method to Study the Optimum Resonator Desitn," 1976 Ultrasonics Symposium Proceedings, pp. 287-296.
3. J. Henaff and P. C. Brossard, "Implementation of Satellite Communication Systems Using SAW; Transaction on Sonics and Ultrasonics. Vol. SU-28, No. 3, pp. 161-172.
4. M. E. Motamedi, A. P. Andrews and E. Brower, "Accelerometer Sensor Using Piezoelctric ZnO Thin Films," 1982 Ultrasonic Symposium Proceedings, pp. 303-306.
5. M. E. Motamedi, A. P. Andrews, T. C. Lim, R. Heatherly, R. S. Muller and P-L. Chen, "A Monolithic Accelerometer for Missile Defense," presented at AIAA Missile and Space Sciences Meeting, September 15, 1982, Monterey, California, (available as NTIS#AD B071700).
6. A. P. Andrews and M. E. Motamedi, "Monolithic Accelerometer," final report, Contract No. DASG60-79-C-0021, September 1983.
7. E. J. Staples, "UHF Surface Acoustic Wave Resonators," Proceedings of the 28th Annual Symposium on Frequency Control, May 1974, pp. 280-285.
8. P. S. Cross, "Reflective Arrats for SAW Resonator," 1975 Ultrasonics Symposium Proceedings, pp. 241-244.
9. B. Y. Lao, N. J. Schneier, D. A. Rowe, R. E. Dietterle, J. S. Schoenwald, E. J. Staples and J. Wise, "SAW Oscillators in UHF Transit Satellite Links," IEEE Trans. on Microwave Theory and Techniques, vol. MTT-29, No. 12, December 1981.
10. M. E. Motamedi, E. J. Staples and J. Wise, "Characterization of ZnO/Si SAW Transducers and Resonators Using Complex Return Loss Measurements," 1981 Ultrasonics Symposium Proceedings, pp. 368-371.

END

FILMED

9-84

DTIC



